Supplementary Information for:

Highly dispersed ultrafine PtCo alloy nanoparticles on unique composite carbon supports for proton exchange membrane fuel cells

Lingling Zhang[a], Tong Liu[a], Xiaokang Liu[a], Sicheng Li[a], Xue Zhang[a], Qiquan Luo[c], Tao Ding*[a,b], Tao Yao[a,b] and Wei Zhang*[a,b]

[a]National Synchrotron Radiation Laboratory, School of Nuclear Science and Technology, University of Science and Technology of China, Hefei 230029, P.R. China

[b]Key Laboratory of Precision and Intelligent Chemistry, Hefei National Research Center for Physical Sciences at the Microscale, University of Science and Technology of China, Hefei 230026, P.R. China.

[c]Institutes of Physical Science and Information Technology, Anhui University, Hefei 230601, China

✉Email: dingtao@ustc.edu.cn; zhangw94@ustc.edu.cn

Content list:

1. Experimental Section

Materials and Chemicals: All the chemicals purchased from commercial sources were used without further purification. Platinum (II) 2,4-pentanedionate ($Pt(acac)_2$), Bis(acetylacetonato)cobalt ($Co(acac)_2$), 2-Methylimidazole, Ethanol (EtOH), Cobaltous nitrate hexahydrate ($Co(NO_3)_2 \cdot 6H_2O$), Methanol (CH_3OH), Acetone (CH_3COCH_3), Sulfuric acid (H_2SO_4), Perchloric acidsodium ($HClO_4$), hypochlorite, Nafion 117 membrane (Dupont) was purchased from Sinero Technology Co., Ltd. Carbon black (Ketjen Black, ECP600JD) were obtained from Suzhou Sinero Technology Co, Itd., Graphite powder (XF0097782-42-5) was obtained from XFNANO Materials Tech Co, Itd.

Synthesis of Ultrafine PtCoNC:

Preparation of carbon support: The carbon support is composed of the NC material derived from Zeolitic Imidazolate Frameworks-67 (ZIF-67) and Ketjen Black (KB). The synthesis process of ZIF-67 particles was as follows: $Co(NO_3)_2 \cdot 6H_2O$ (873.9 mg, 3 mmol) and 2- methylimidazole (2-MeIm, 985.7 mg, 12 mmol) were, respectively, dissolved in 20 mL of methanol to form clear solutions; the prepared Co^{2+} containing solution was slowly added into 2-MeIm solution and stirred; the mixed solution was maintained at 60 °C for 1 h; the resulting ZIF-67 precipitates were collected by centrifugation, washed with ethanol for several times, and dried at 60 °C in the vacuum oven for 24 h. Then, the as-synthesized ZIF-67 was poured into a tube furnace and heated to 900 °C at a ramp rate of 5 °C min^{-1} and kept for 1 h in N_2 flow. The furnace was then cooled naturally to room temperature (25 °C) to obtain ZIF-67NC black powder. The Ketjen Black was heated to 800 °C at a ramp rate of 5 °C min^{-1} and kept for 2 h in N_2 flow in a 10 vol% H_2/Ar flow. Then, the two carbon were fully mixed and ground as composite support. The mass ratio of ZIF-67NC to KB is 1:2.

Synthesis of PtCoNC: Typically, 50 mg $Pt(acac)_2$ and 15mg $Co(acac)_2$ were dissolved in 20 mL acetone. The mixture was ultrasonicated to form clear solutions, which is then added to as-prepared carbon support. And, the mass ratio of ZIF-67NC to KB is 1:2 of carbon support. Then, the mixed solution was ultrasonicated for 3 h at room temperature

until well combined. After removing the solvent by rotary evaporator at 35 °C, the black mixture powder was collected. After that, the precursor was annealed in 10% H_2/Ar atmosphere at 700 °C for 6 h to obtain the ultrafine nanoparticle. Acid wash and annealing: Afterwards, the synthesized PtCoNC was acid etched at 85 °C for 16 h in N_2-saturated 0.2 M H_2SO_4. After the acid etched, collected catalyst via centrifugation, the catalyst was washed a few times with ultrapure water. And then, the obtained catalyst was annealed in a 10% H_2/Ar mixture at 200 °C for 1.5 h. The final product was collected until it had fully cooled down. For a fair comparison, the synthesis procedure is similar with the PtCoNC. The only difference is using other carbon base to load PtCo alloy.

Characterization methods: Transmission electron microscopy (TEM) analysis was performed on a JEOL−2100F transmission electron microscope at an accelerating voltage of 200 kV. Energy dispersive spectra (EDS−mapping) were performed on a F200 transmission electron microscope at an accelerating voltage of 200 kV. The X−ray photoelectron spectra (XPS) were recorded on a Thermo ESCALAB250Xi spectrometer with an excitation source of monochromatized Al Kα (hν = 1486.6 eV) and a pass energy of 30 eV. The values of binding energies were calibrated with the C 1s peak of contaminant carbon at 284.80 eV. X−ray diffraction (XRD) patterns were was carried out on a Rigaku miniflex600 diffractometer. Elements quantitative analysis were carried out by an inductively coupled plasma atomic emission spectroscopy (ICP−AES) analysis of PerkinElmer Model Optima 3000DV. Raman spectroscopy analysis was carried out on a confocal Raman spectrometer (LabRAM HR Evolution) with a wavelength of 532 nm. The contact angle measurement was carried out on JY-82C. The in-situ SRIR tests were performed at the BL01B at NSRL with a home-made electrochemical IR cell.

XAS measurement: The Pt L_3-edge (11,564 eV) XAFS spectra were measured at the 1W1B beamline of Beijing Synchrotron Radiation Facility (BSRF), China. The storage

ring of BSRF was operated at 2.5 GeV with a maximum electron current of 250 mA. The hard X-ray was monochromatized with a Si (111) double crystal monochromator and detuned by 30% to remove harmonics. Operando XAFS measurements were performed in the fluorescence mode. Position of the absorption edge (E_0) was calibrated using Pt foil. The electrochemical in situ XAFS tests were performed by a homemade cell in a 0.1 M $HClO_4$ electrolyte. To obtain the evolution information of the active site during the electrochemical reaction, a series of representative potentials were applied to the electrode. The MEA test bench uses Scribner 850e.

Electrochemical measurements and PEMFC performance test:

The electrochemical measurements were carried out by a CHI 660 electrochemical workstation with a rotating ring-disk electrode (RRDE) assemble (MSR, Pine Research Instrumentation, USA) in 0.1 M $HClO_4$. A rotating disk electrode (RDE) or RRDE of 5 mm in diameter loaded with the catalyst ink was used as working electrode. An Ag/AgCl (saturated KCl) electrode and a carbon rod were served as reference and counter electrode, respectively. Catalysts inks used in the electrochemical measurements were prepared by dispersing 2 mg of catalyst powder in the mixture solution (0.50 mL ethanol, 0.48 mL deionized water, 20 μL Nafion) and then sonicating to form homogeneous catalyst inks. The as-prepared ink is dropped onto glassy carbon（GC）disk of the RDE or RRDE 8~12 μL according to film forming quality. The catalyst loading on the RDE and RRDE electrodes is about 0.1 mg cm^{-2}. The Pt loading is almost 28.6 μg mL^{-1}. The RDE/RRDE tests were measured at various rotating speed from 400 to 2500 rpm in O_2-saturated 0.1M $HClO_4$ aqueous solution with a sweep rate of 10 mV/s. The hydrogen peroxide yield (H_2O_2 %) and average electron transfer number based on RRDE measurements can be determined by the following equations;

$$H_2O_2\ (\%) = 200 \times \frac{Ir/N}{Id + Ir/N}$$

$$n = 4 \times \frac{Id}{Id + Ir/N}$$

where I_d is the disk current, I_r is the ring current, and N = 0.37 is the current collection efficiency of the Pt ring. All potentials were calibrated vs. RHE.

$$E(RHE) = E(Ag/AgCl) + 0.197\ V + 0.059\ pH$$

Gas diffusion electrode preparation: All Membrane Electrode Assemblies (MEAs) were prepared by ultrasonic spraying. The catalyst and the ionomer (D520, 5wt.%, EW1100) were dispersed in a mixture of water and ethanol with a certain proportion (1:1). Then the ink for ultrasonic spraying was prepared by ultrasound in an ice bath for 1 h. Ready to spray：After cleaning the pipeline, use a syringe to load the ink； and determine the spraying amount and adjust the flow rate; set the spray parameters and determine the starting position, select the spray mode. Reset, test spray, finish and start spraying procedure. PEMFC test: Commercial Johnson Matthey Hispec 3000 was used for the anode and PtCoNC prepared for the cathode. The anode load of precious metal is 0.05 $mg_{Pt}\,cm^{-2}$, the cathode is 0.15 $mg_{Pt}\,cm^{-2}$, and the area is 5 cm^2. The GDL and the prepared CCM were fixed on the prepared PTFE substrate to form the MEAs. The PTFE substrate thickness was 160 μm to ensure that the compression rate of the GDL was 75-80%. Before the polarization curve test, use a large flow of pure nitrogen to purge the cathode and anode for more than 20 minutes to eliminate residual air in the battery. Pure oxygen and pure hydrogen as cathode and anode reactant, respectively. When cathode less than 0.2 A cm^{-2} uses a fixed flow rate (Anode:10 sccm, Anode: 14 sccm), whereas larger than 0.2 A cm^{-2} uses a metering ratio (Anode:1.5, cathode:4.0). The dew point and operating temperature are set as 80 °C, 100%RH and the back pressure is 200 Kpa.abs. The cell voltage is stabilized at 0.7 V and 0.5 V for 20 min respectively. And the cycle is repeated 5 times to achieve the activation of MEAs. Before conducting the polarization curve test, perform a cathode starvation step and use pure nitrogen to blow the cathode, reducing the battery voltage to less than 0.1V. Increase the current density by 0.2 A cm^{-2} from 0 to 4 A cm^{-2} and maintain each point for 3 minutes to record data.

Operando synchrotron−radiation Fourier transform infrared spectroscopy (SR−FTIR) measurements: Operando SR−FTIR measurements were made at the infrared beamline BL01B of the National Synchrotron Radiation Laboratory (NSRL), China, through a homemade top−plate cell reflection infrared set−up with a ZnSe crystal as the infrared transmission window (cut−off energy of ~625 cm^{-1}). This end station was equipped with an FTIR spectrometer (Bruker IFS 66 v/s) with a KBr beam splitter and various detectors (herein a liquid nitrogen cooled mercury cadmium telluride detector was used) coupled with an infrared microscope (Bruker Hyperion 3000) with a ×16 objective, and could provide infrared spectroscopy measurement with a broad range of 15−4000 cm^{-1} as well as a high spectral resolution of 0.25 cm^{-1}. The catalyst electrode was tightly pressed against the ZnSe crystal window with a micrometre−scale gap in order to reduce the loss of infrared light. Each infrared absorption spectrum was acquired by averaging 514 scans at a resolution of 2 cm^{-1}. The background spectrum of the catalyst electrode was acquired at an open−circuit voltage before each systemic measurement, and the measured potential ranges of the electrocoupling reaction were 1.0 −0.05 V.

Calculation details: The calculations were performed within the Density Functional Theory (DFT) framework implanted in Vienna ab initio Simulation Package (VASP)[2] The interaction between ions and electrons was described in the Projector Augmented Wave (PAW) Method[1]. The electron exchange and correlation energy were described using the generalized gradient approximation-based Perdew–Burke–Erzenhorf (PBE) functional[2]. The semi-empirical London dispersion corrections of Grimme and colleagues (DFT-D3) were conducted to calculate the interactions between absorbers and slabs[3]. The models of PtCoNC and PtC with a (7 × 7 × 1) graphene supercell were built. A sufficiently large vacuum region of 15 Å was used for all the models to ensure the periodic images were well separated. The Brillouin-zone integrations were carried out using Monkhorst-Pack grids of special points. A gamma-centered (2 × 2 × 1) k-

point grid were used for supercell. To obtain the accurate structure, the plane-wave cutoff energy was set up to 500 eV. The force convergence was set to be <0.02 eV $Å^{-1}$, and the total energy convergence was set to be $<10^{-5}$ eV. The free energy of the adsorbed state was calculated as follows based on the adsorption energy:

$$\Delta G^* = \Delta E^* + \Delta EZPE + U(T) - T\Delta S$$

where ΔE^* is the adsorption energy directly obtained from DFT calculations, $\Delta EZPE$ is the zero-point energy, U(T) is the heat capacity correction energy, and T is the temperature (T = 298.15 K), ΔS is the change in entropy. Herein, the Gibbs energy is corrected by using the VASPKIT code[4].

2. Experimental Section

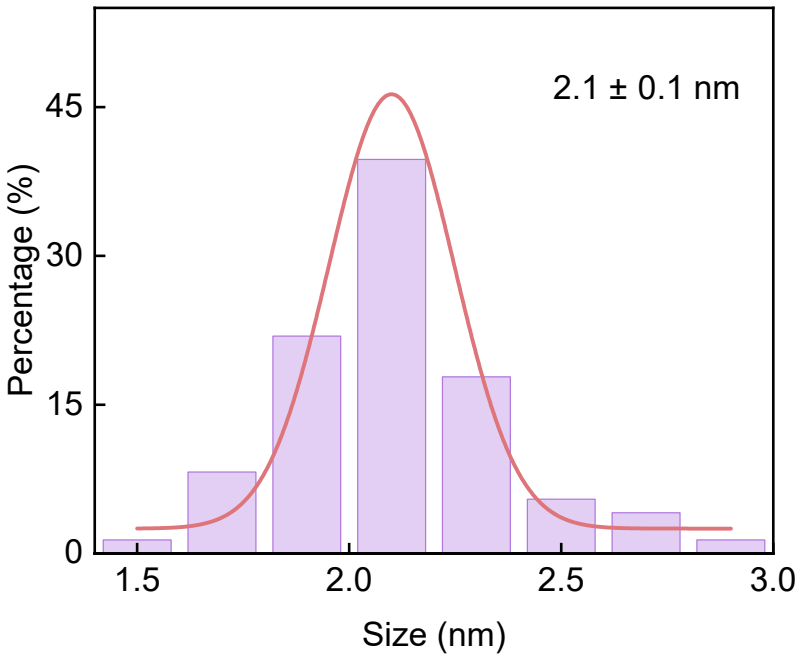

Supplementary Figure 1. Size distribution of PtCoNC.

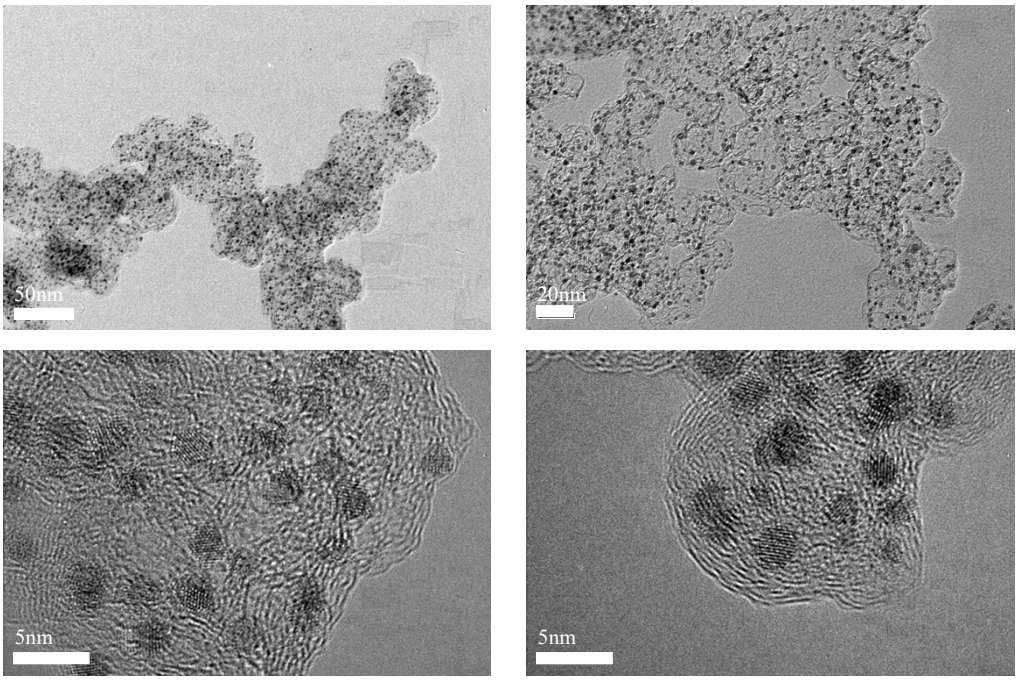

Supplementary Figure 2. TEM and HRTEM images of PtCoNC.

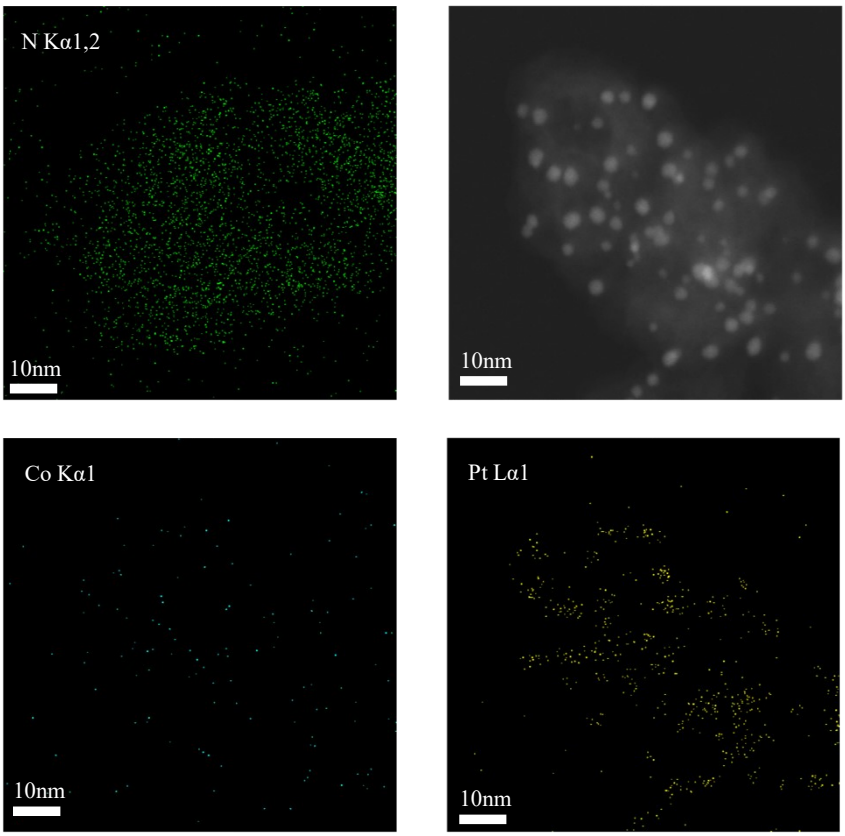

Supplementary Figure 3. EDS mapping of PtCoNC.

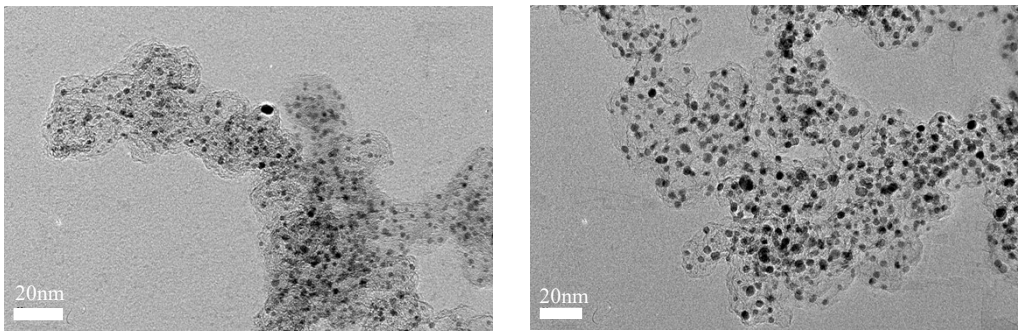

Supplementary Figure 4. TEM images of PtCoKB.

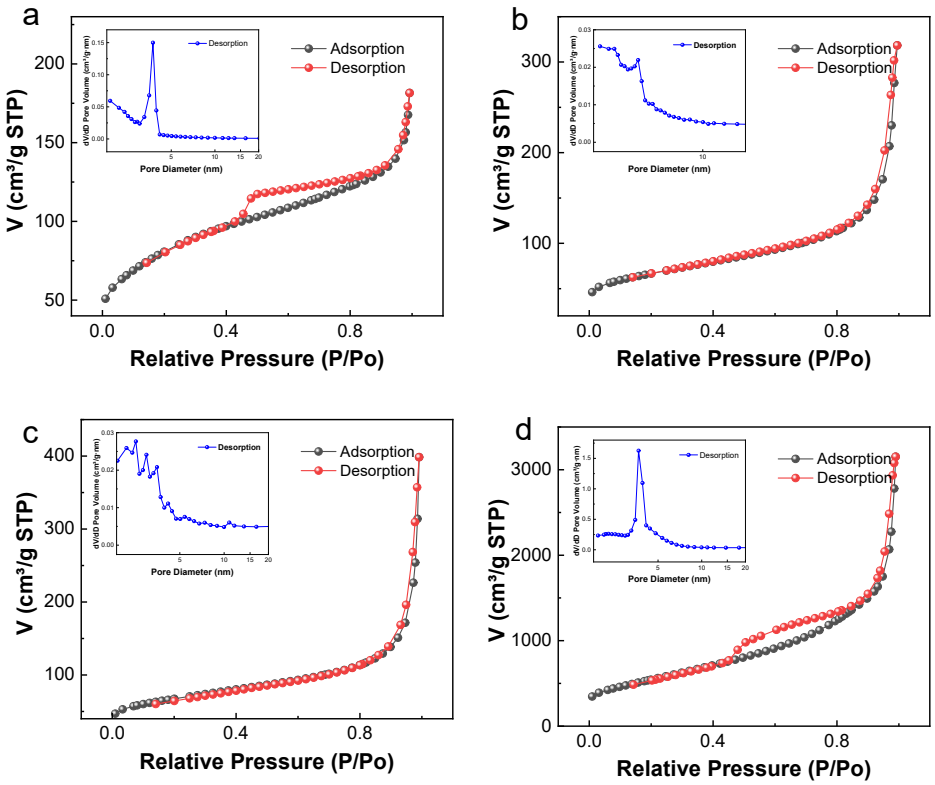

Supplementary Figure 5. The BET and pore distribution analysis of (a) PtCoZIF67-NC, (b) PtCoXC-72, (c) PtCoVC-72 and (d) Ketjen black support.

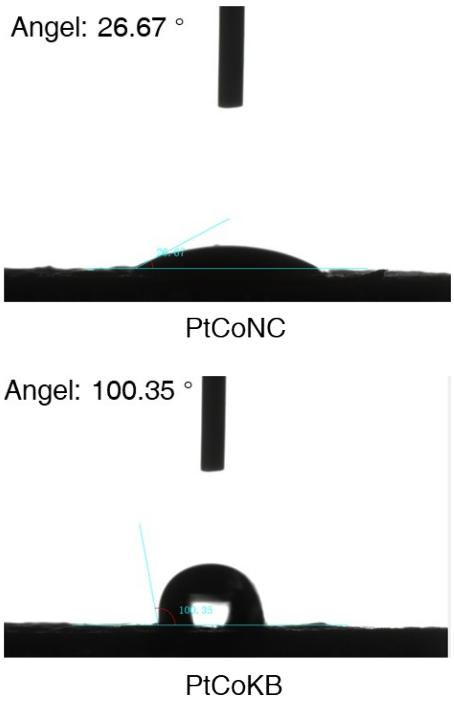

Supplementary Figure 6. Photographs of contact angle measurements of PtCoNC and PtCoKB.

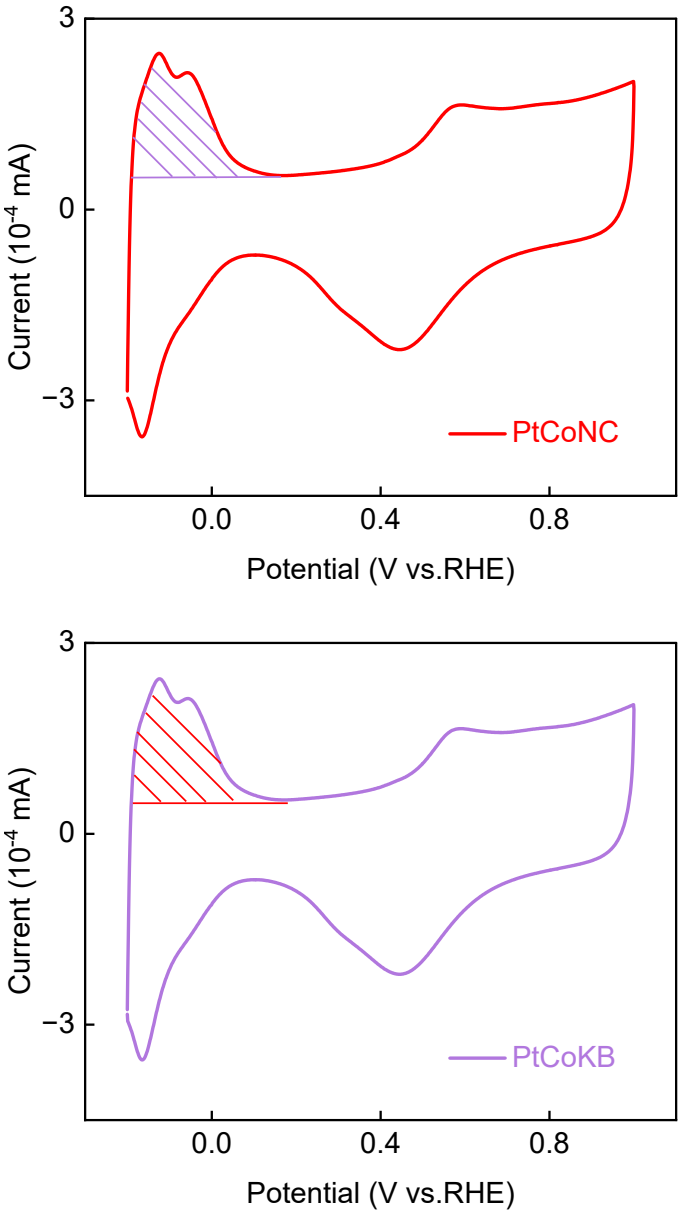

Supplementary Figure 7. The ECSA of PtCoNC and PtCoKB.

Note 1: Calculation of Roughness Factor (RF)[10]

The roughness factor (RF) is calculated via taking the estimated ECSA and dividing by the geometric area of the electrode (Ag = 0.196 cm^2), and according to the :

$$RF=ESCA/Ag$$

Note 2: Calculation of ECSA

The ECSA values were calculated by integrating the hydrogen adsorption charge in the voltammogram (0.05 to 0.35 V), 210 μC/cm^2 (theoretical hydrogen monolayer adsorption on Pt) and the cathode initial Pt loading (mg_{Pt}/cm^2):

$$ECSA=Q_H/0.21$$

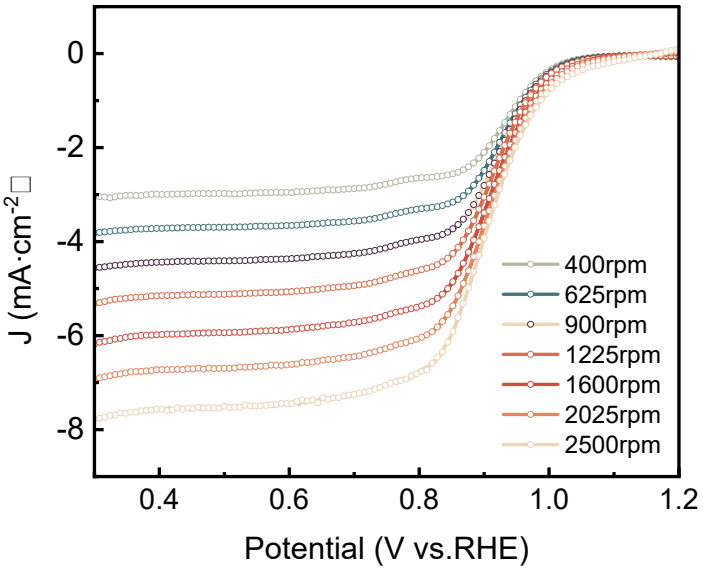

Supplementary Figure 8. The LSV curves of different rotating rates.

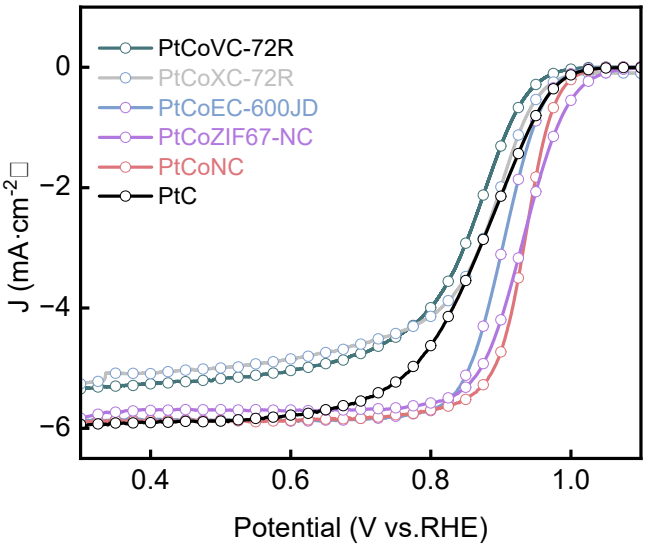

Supplementary Figure 9. The LSV curves of typical carbon carrier loaded PtCo.

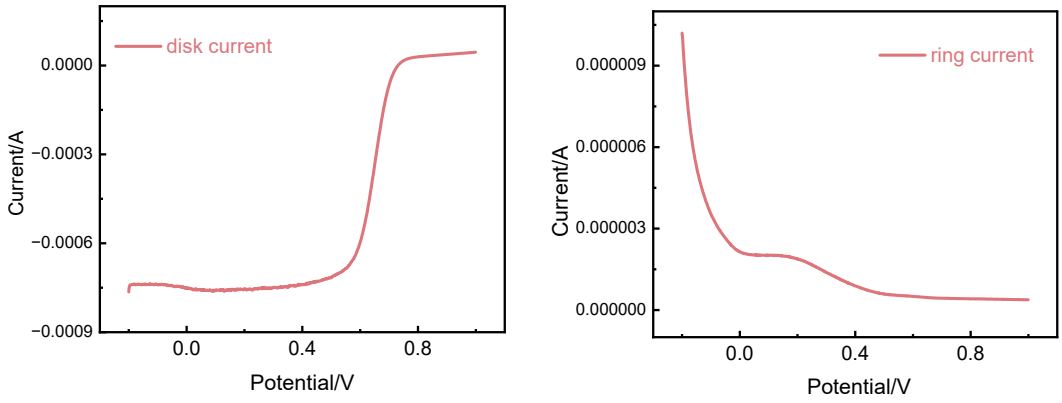

Supplementary Figure 10. Ring disk electrode test results of PtCoNC.

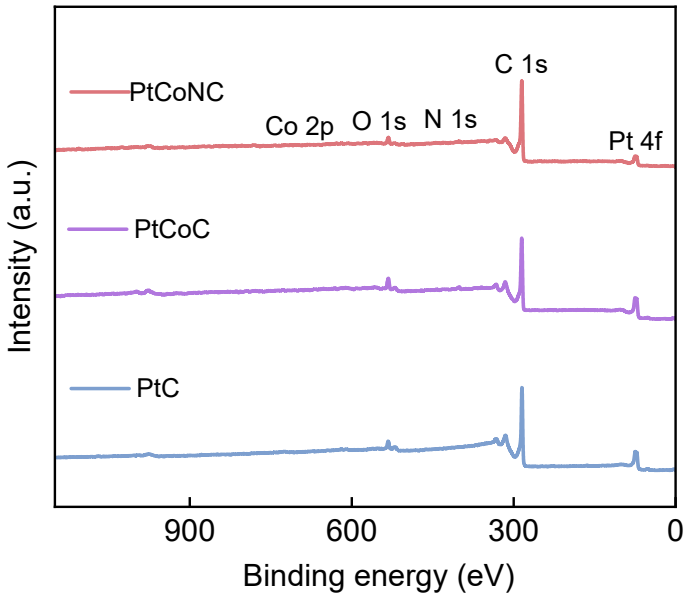

Supplementary Figure 11. XPS spectra for PtCoNC, PtCoKB and PtCoZIF67.

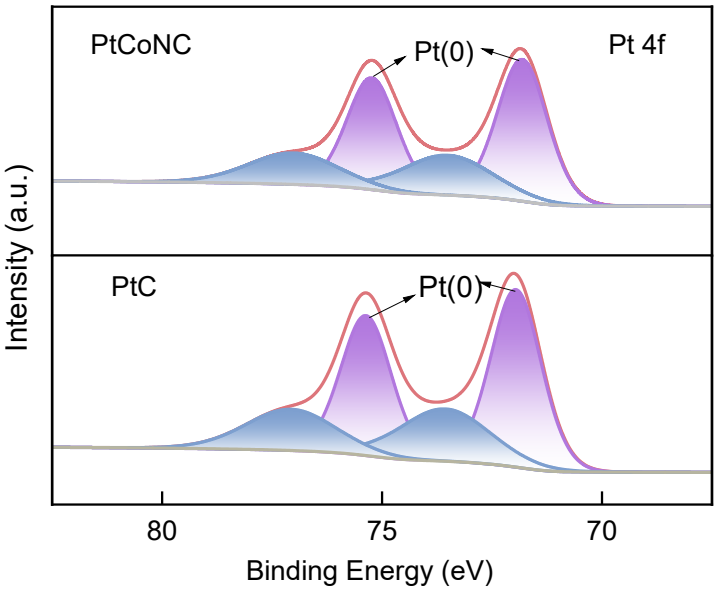

Supplementary Figure 12. Pt 4f XPS spectra for PtCoNC.

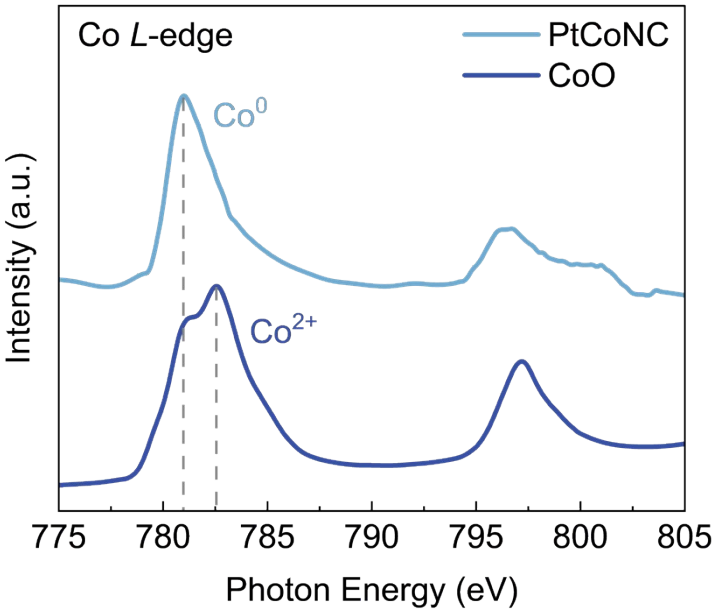

Supplementary Figure 13. Co *L*-edge XAS spectra for PtCoNC and CoO.

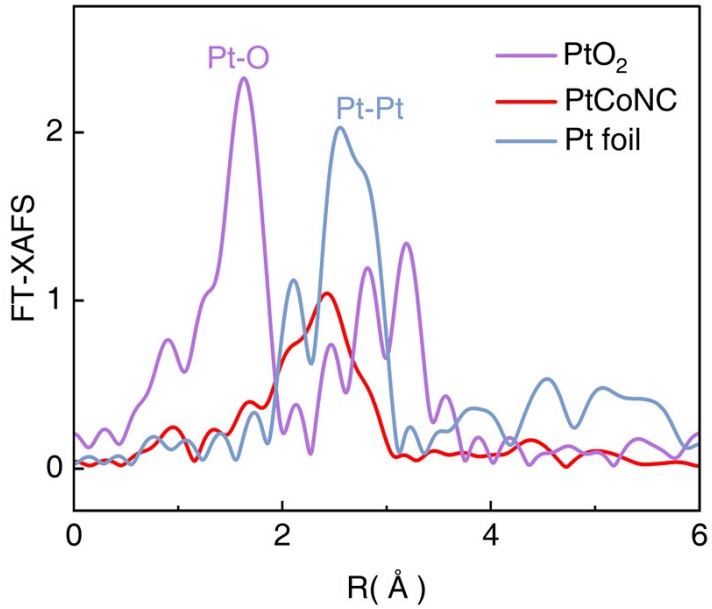

Supplementary Figure 14. The corresponding k^2-weighted FT-XAFS spectra.

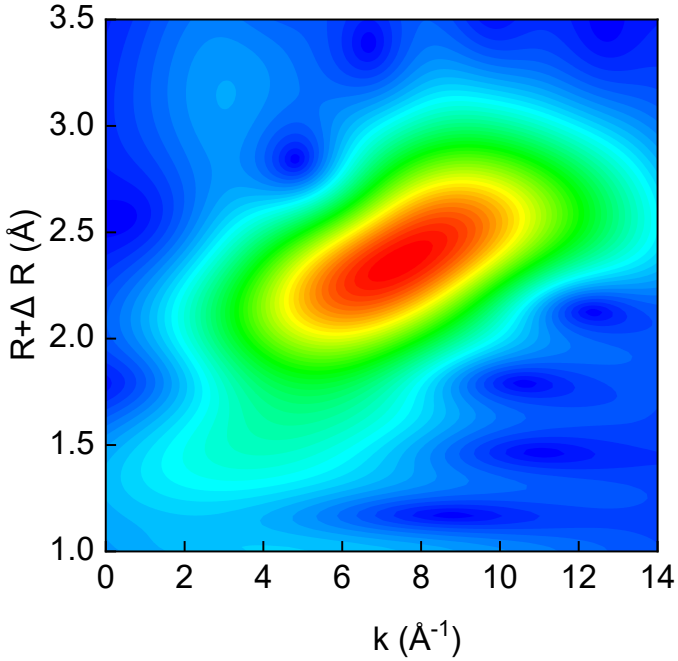

Supplementary Figure 15. Wavelet transforms (WT) for PtCoNC.

.

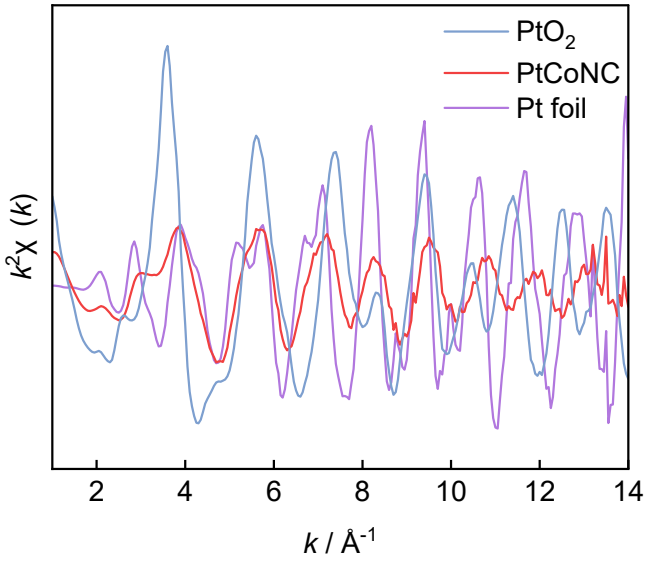

Supplementary Figure 16. $K^2\chi$(k) oscillations of the Pt L_3–edge EXAFS signals for Pt foil, PtCoNC and PtO_2.

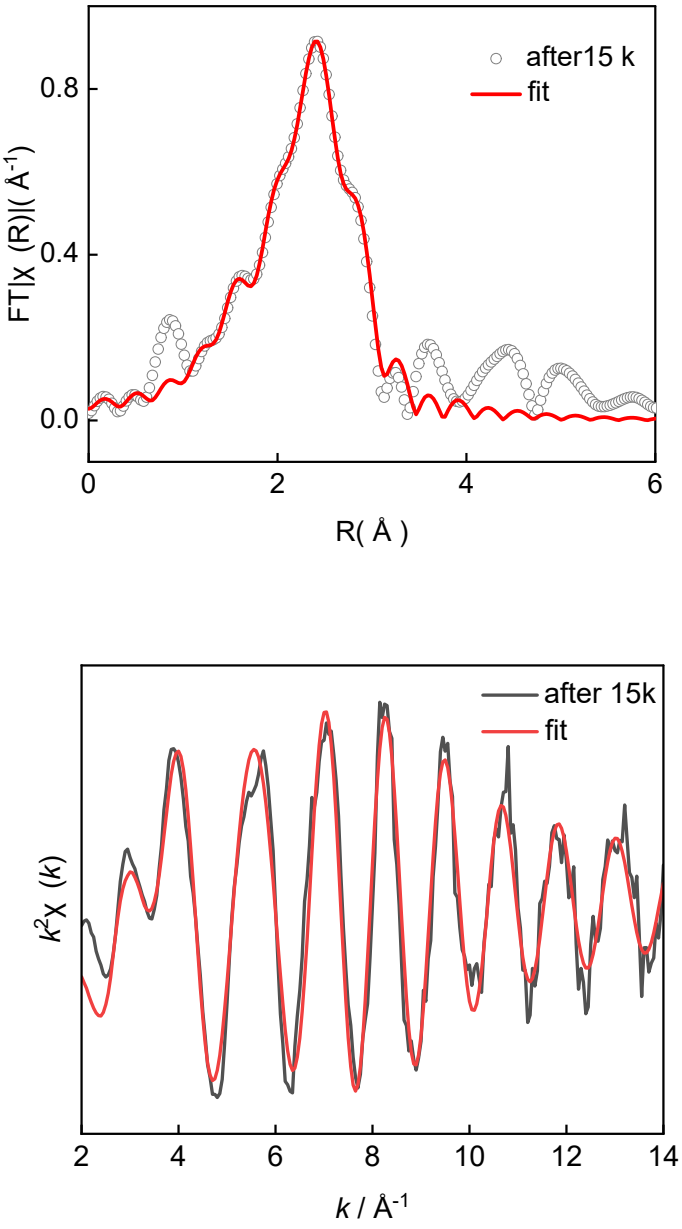

Supplementary Figure 17. Least-squares curve-fitting analysis of EXAFS spectra at the Pt L_3-edge and corresponding Re[$k^2\chi(k)$] oscillations.

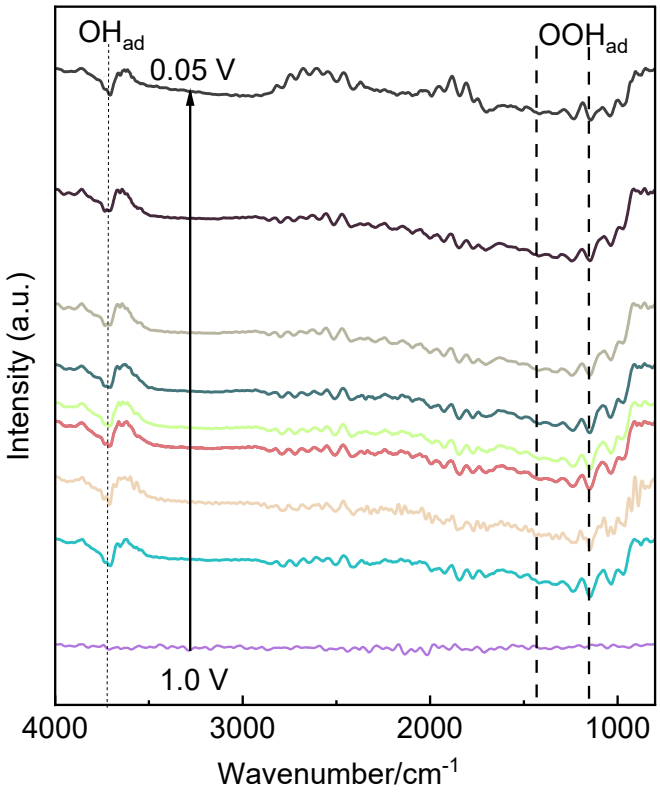

Supplementary Figure 18. The operando SR-FTIR spectra for PtCoNC.

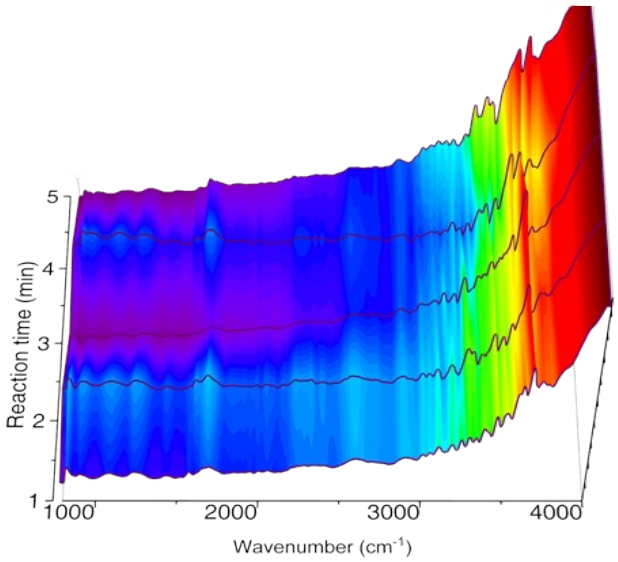

Supplementary Figure 19. The operando SR-FTIR spectra showing water formation during the ORR at 0.93 V vs. RHE in 0.1 M $HClO_4$.

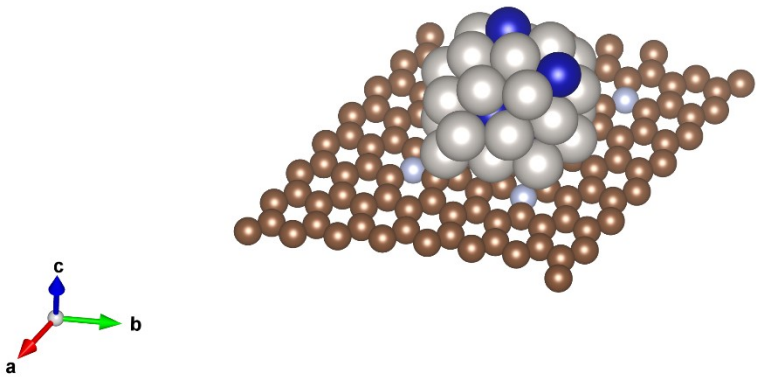

Supplementary Figure 20. A computational model N–doped carbon loaded with PtCo clusters.

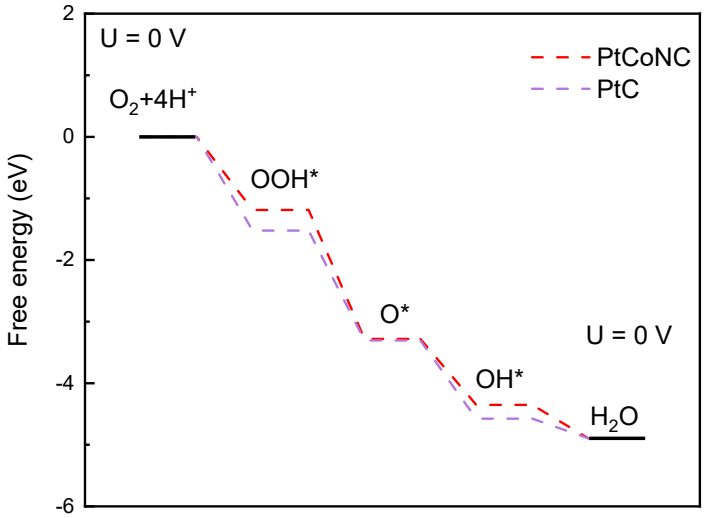

Supplementary Figure 21. ORR energy profiles on the series of geometry-optimized PtCo slabs at U = 0 V.

3 Supplementary Tables

Table S1. The physical properties of samples by t-plot analysis.

Sample	Average pore size (nm)	$S_{BET(}m^2 \cdot g^{-1})$		Pore volume($cm^3 \cdot g^{-1}$)	
		micropores	meso-macropores	micropores	meso-macropores
PtCoKB	8.71	17.2	1957.5	0.002	4.977
PtCoXC-72R	12.8	65.4	161.2	0.032	0.413
PtCoZIF-67NC	4.87	29.2	255.1	0.013	0.219
PtCoVC-72R	16.1	66.8	161.8	0.033	0.541
PtCoNC	7.57	32.3	1314.5	0.006	2.060

Table S2. Structural parameters of PtCoNC at the Pt L_3-edge extracted from quantitative EXAFS curve-fittings using the ARTEMIS module of IFEFFIT.

Sample	Path	CN	R(Å)	σ^2 (10^{-3})	ΔE_0(eV)	R-factor
	Pt-O/N	0.8	2.01	5.0	9.81	
In air	Pt-Co	1.6	2.64	5.4	6.72	0.004
	Pt-Pt	5.7	2.72	6.1	6.33	
	Pt-O/N	1.0	2.04	6.0	9.70	
1.0 V	Pt-Co	1.6	2.63	6.2	4.05	0.008
	Pt-Pt	6.3	2.72	6.8	6.80	
	Pt-O/N	0.8	2.01	5.0	9.81	
0.93 V	Pt-Co	1.6	2.64	5.4	6.72	0.002
	Pt-Pt	5.7	2.72	6.1	6.33	
	0.7	2.01	5.0	10.0	0.7	
0.6 V	1.7	2.65	6.1	7.62	1.7	0.009
	6.1	2.71	6.5	5.41	6.1	
After	0.88	1.98	6.0	7.51	0.88	
reaction	1.7	2.65	9.2	7.93	1.7	0.006
	6.4	2.72	6.6	6.33	6.4	

S_0^2 was fixed as 0.82. Data ranges: $2.8 \leq k \leq 12.7$ Å, $1.0 < R < 3.0$ Å. The number of variable parameters is 9.3, out of a total of 12 independent data points. The distances for Pt-O are from the crystal structure of Pt_3O_4; The distance of Pt-Pt is from the FEFF file of PtCo; The distance of Pt-Co is from the FEFF file of Pt_3Co.

Table S3. The peak table from XPS test of PtCoNC.

Name	FWHM eV	Area (P) CPS. eV	Atomic %	PP At. %
Pt 4f	1.52	16578.87	1.08	0.59
C 1s	0.89	54109.62	62.02	69.4
C 1s Scan A	2.25	25961.95	29.76	27.09
N 1s	1.8	3226.69	2.29	1.45
O 1s	2.83	10305.16	4.46	1.39
Co 2p	1.34	5041.41	0.39	0.07

4 References

(1). H. Gao, J. Zang, X. Liu, Y. Wang, P. Tian, S. Zhou, S. Song, P. Chen and W. Li, *Appl. Surf. Sci*., 2019, **494**, 101−110.
(2). L. Cao, Q. Luo, J. Chen, L. Wang, Y. Lin, H. Wang, X. Liu, X. Shen, W. Zhang, W. Liu, Z. Qi, Z. Jiang, J. Yang and T. Yao, *Nat. Commun*., 2019, **10**, 4849.
(3). P. E. Blöchl, *Phys. Rev. B*., 1994, **50**, 17953−17979.
(4). John P. Perdew, Kieron Burke and M. Ernzerhof, *Phys. Rev. Lett.,* 1996, **77**, 3865–3868.
(5). S. Grimme, *J Comput Chem*., 2006, **21**, 1787−1799.
(6). Vei Wang; Nan Xu; Jin-Cheng Liu; Gang Tang; Geng, W.-T., *Comput Phys Commun*., 2021, **267**, 108033.
(7). M. Newville, *J. Synchrotron Radiat*., 2001, **8**, 322−324.
(8). B. Ravel, M. Newville, *J. Synchrotron Radiat*., 2005, **12**, 537−541.
(9). A. L. Ankudinov, B. Ravel, J. J. Rehr, S. D. *Conradson, Phys. Rev. B*., 1998, **58**, 7565−7576.